

Template-Free Parallel One-Dimensional Assembly of Gold Nanoparticles

Yu Xin Zhang and Hua Chun Zeng*

*Department of Chemical and Biomolecular Engineering, Faculty of Engineering,
National University of Singapore, 10 Kent Ridge Crescent, Singapore 119260*

Received: June 8, 2006; In Final Form: July 25, 2006

In this work, we have identified key process parameters to generate parallel unidirectional 1D assemblies of gold nanoparticles with the assistance of organic surfactants. By controlling the surfactant population, metal particle size, and amount of solvent for dispersion, the length of nanoparticle chains and their interchain space can be further tailored. In principle, the general findings of this work can also be extended to large-scale 1D organization of other transition/noble metal nanoparticles using simple organic surfactants.

Introduction

One-, two-, and three-dimensional (1D, 2D, and 3D) assemblies of nanoparticles (0D) have become a subject of active research in recent years.^{1–7} As an important noble metal, for example, nanosized gold (Au) particles in different geometrical forms have been recently synthesized and organized into various superlattices and superstructures.^{2,5,7} With their pseudospherical shapes, the Au nanoparticles can self-assemble into stable and ordered constructs with assistance of surfactants, ligands, and templates. In comparison to 2D and 3D assemblies, which are commonly in the forms of square and hexagonal arrangements or stacks,^{5,7} 1D assembly of Au nanoparticles is much more difficult to pursue, because the (0D) nanoparticles normally do not exhibit distinct intrinsic anisotropies, noting that gold has a face-centered cubic (fcc) crystal structure. To circumvent this difficulty, various organizing strategies have been developed, mostly templating techniques, in which biomolecules (e.g., DNA), polyelectrolytes, nanotubes, fibers, liquid–solid–air interface (a Langmuir–Blodgett method), and prescribed line substrates, and so forth, have been successfully utilized.² Concerning a next-phase research in this area, template-free 1D assembly of metal nanoparticles would be highly desirable. As an excellent example in this emerging new research, a facile self-assembly of Au nanoparticles into branched chain networks had been very recently realized through surface ligand exchange.^{3a} Nonetheless, without the guidance of prepatterned hard templates, straight, well-ordered, unbranched 1D assembly of Au nanoparticles with a precise interparticle distance has remained unsuccessful so far.³ In this letter, we report an investigation on 1D self-assembly of Au nanoparticles via manipulating surface ligand content, particle size, and dispersive concentration. With the present template-free approach, stable parallel 1D assemblies of Au nanoparticles have been obtained for the first time.

Experimental Section

The As-Prepared Samples. In a typical synthesis, Au nanoparticles were prepared according to Brust's two-phase

reaction procedure with some minor modifications. Briefly, the hydrogen tetrachloroaurate trihydrate ($\text{HAuCl}_4 \cdot 3\text{H}_2\text{O}$) aqueous solution (32.85 mM, 3.0 mL) was added to tetraoctylammonium bromide (TOAB) in toluene (49.5 mM, 3.982 mL), and the mixture was vigorously stirred. The yellow aqueous solution became colorless, and the toluene phase turned orange as a result of the transformation of $[\text{AuCl}_4]^-$ with TOAB cations. After stirring the solution mixed with 1-dodecanethiol (DT) in toluene (0.1106 M, 0.4455 mL) for 15 min at room temperature, a freshly prepared aqueous solution (0.4457 M, 2.2 mL) of sodium borohydride (NaBH_4) was added to the vigorously stirred solution. The resulting solution immediately turned from orange to deep brown and continued to be stirred for 15 min. The organic phase (about 4.43 mL) was evaporated inside a vacuum container at room temperature, and the solid product obtained at this stage is termed as “the as-prepared Au nanoparticles” in the main text.

The Ethanol-Washed Samples. In another process method studied in this work, the same organic phase (about 4.43 mL) obtained from the above was mixed with 30 mL of ethanol to remove excess organic ligands (i.e., TOAB and DT). The dark brown precipitate in ethanol was separated by centrifuging at 5000 rpm for 10 min. The crude product was dissolved in 3 mL toluene and again precipitated with 30 mL ethanol. After the same centrifuging separation and air-drying at room temperature, the products are called as “the ethanol-washed Au nanoparticles” in the main text. In some cases, up to three washing cycles were performed.

The Heat-Treated Samples. The heat treatments for the Au nanoparticles were carried out in a quartz tube furnace operated under normal atmospheric ambience. The heating rate was selected in the range 2–10 °C per minute. When reaching a desired temperature (130–300 °C), the samples were held at the same temperature for 30 to 120 min, followed by natural cooling to room temperature. The products are called as “the heated Au nanoparticles” in the main text.

The Toluene-Diluted Samples. In preparation of suspensions of Au nanoparticles for TEM/HRTEM analysis, 0.5–2.5 mg of the above samples was added into 3–12 mL of toluene in an ultrasonic bath. One or two drops of the as-prepared

* Tel: (65) 6516-2896. Fax: (65) 6779-1936. Email: chezhc@nus.edu.sg.

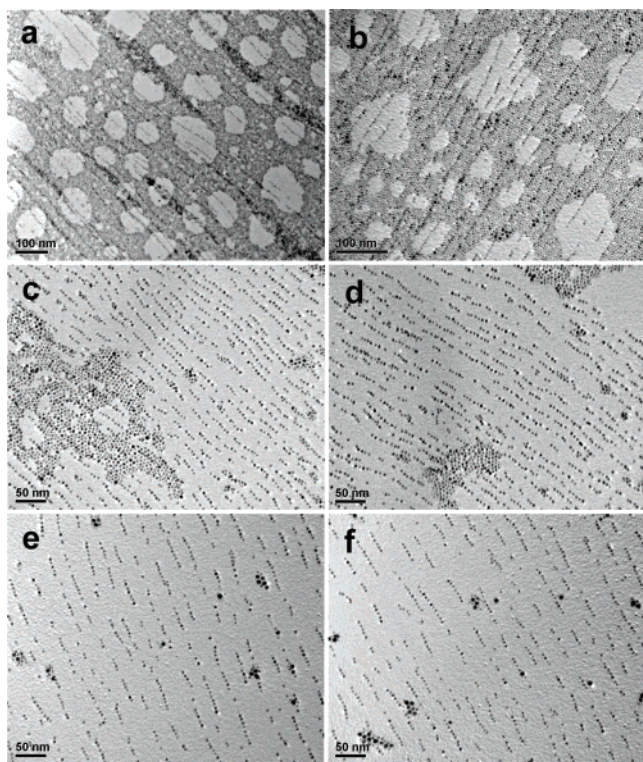


Figure 1. TEM images of 1D assemblies of Au nanoparticles (ethanol washed and 150 °C heat-treated) in toluene solvent: normal suspension (a,b), diluted suspension (c,d), and more dilute suspension (e,f).

suspensions were placed onto holey carbon films supported on standard copper grids. After toluene evaporation, the specimens were ready for examinations by TEM/HRTEM/SAED methods.

Materials Characterization. The prepared materials were characterized with transmission electron microscopy (TEM, JEM-2010F), high-resolution TEM, and selected area electron diffraction (HRTEM/SAED, Philips-CM200 FEG), a combined scanning TEM and field emission scanning electron microscopy (STEM/FESEM/EDX; JSM-6700F), Fourier transform infrared spectroscopy (FTIR, Bio-Rad FTS 135), elemental analysis (Perkin-Elmer 2400 CHNS analyzer), and X-ray photoelectron spectroscopy (XPS; AXIS-HSi, Kratos Analytical).

Results and Discussion

Figure 1 presents three sets of 1D assemblies of the 150 °C-heated Au nanoparticles in toluene solvent. When the Au particle concentration is high, two-dimensional hexagonal arrays are formed together with basinlike voids. Quite surprisingly, parallel-line assemblies of the Au nanoparticles are also aligned across the surfaces. These particle lines are smooth and stable, extending several micrometers without breaking their linearity. In particular, the threadlike assemblies are not interrupted by the substrates when they are climbing up from the uncovered sample grid to the terrace of the 2D Au aggregates, noting that the both substrates (i.e., the uncovered grid area and the 2D aggregates) have similar hydrophobic natures. Nonetheless, this particle–substrate interaction is rather weak. It is noted that there is no definite relationships between the hexagonal 2D arrays and the line assemblies, as detailed in Figure 2a, which suggests that the lined particles may be simply formed in a more dilute suspension after the process of 2D sedimentation. A combined investigation using both STEM and FESEM techniques indicates that the structural effect of pristine TEM sample grid on the observed assemblies can be ruled out (Supporting

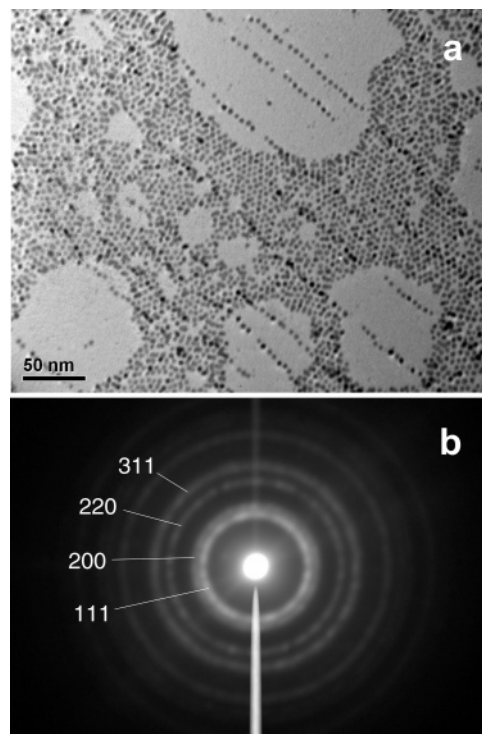


Figure 2. TEM image (a) and its corresponding SAED pattern (b) measured for Au nanoparticles synthesized after heating at 150 °C (see Experimental Section).

Information, SI-1). Indeed, the parallel arrangement with constant interline spaces confirms that these 1D assemblies are coexisting prior to the drying, i.e., the linear engagement among the Au particles has been established in the solution phase. Consistent with these observations, the 2D arrays become lesser with more toluene in the suspensions, as shown in Figure 1c,d. Despite shorter lengths, the linear interconnectivity among different smaller segments is still maintained. At an even lower concentration of Au (Figure 1e,f), the 1D assemblies of Au nanoparticles become predominant, accompanied by a small amount of tiny 2D islands formed merely from larger Au nanoparticles.

The above observations can be attributed to the factors tested in this work: (i) controlling surface population of capping ligands via washing the as-synthesized Au nanoparticles with ethanol, (ii) tuning the size of Au nanoparticles by heating, and (iii) diluting the Au nanoparticles in toluene to generate the 1D organization. Without ethanol washing, for instance, the as-prepared Au nanoparticles always give 2D hexagonal arrangements, and they have an average size of 2.2 ± 0.7 nm. When they are heated at 150 °C, on the other hand, the nanoparticles can be grown into larger ones,^{5e,f} whose size is increased to 3.6 ± 0.6 nm.

The crystallographic structure of the Au nanoparticles is verified with the SAED investigation reported in Figure 2. As small spherical Au nanoparticles normally possess {111} facets (e.g., cuboctahedron and decahedron, etc.), the {111} ring is more pronounced in the diffraction pattern. Our FTIR investigation of Figure 3a shows that both DT and TOAB are present on the as-prepared Au nanoparticles, since the spectrum of this sample shows a superimposition of the fingerprint vibrations of the two compounds. This IR study also indicates that ethanol washing is an efficient means to remove excess organic surfactants. For example, C–H vibrational modes located at 2920 and 2850 cm^{-1} [$\nu_{\text{as}}(\text{CH}_2)$ and $\nu_{\text{s}}(\text{CH}_2)$] and weaker modes at 2962 and 2878 cm^{-1} [$\nu_{\text{as}}(\text{CH}_3)$ and $\nu_{\text{s}}(\text{CH}_3)$] of the surface-

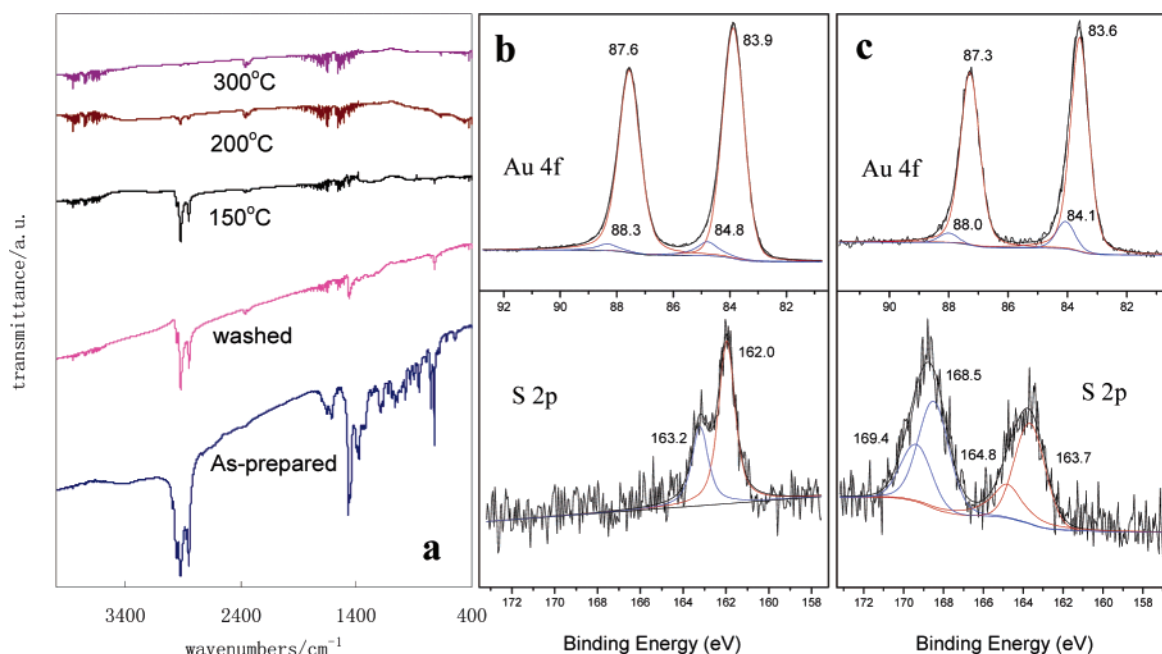


Figure 3. FTIR spectra (a) of the as-prepared, ethanol-washed, and heated Au nanoparticles (Supporting Information SI-2), and XPS spectra of Au 4f and S 2p photoelectrons of the Au nanoparticles heated at 150 °C (b) and 200 °C (c).

TABLE 1: Elemental Analysis of the Studied Au Nanoparticles

sample	C%	H%	N%	S%
as-prepared	59.47	11.03	2.33	2.61
ethanol-washed	17.84	2.90	0.36	4.09
150 °C-heated	16.96	2.81	0.33	4.20
200 °C-heated	6.48	0.97	0.38	1.36

adsorbed ligands have been significantly reduced after washing (Supporting Information, SI-2). At a moderate temperature (e.g., 150 °C under the ambient conditions), these organic species are still kept on the Au surfaces, which leads to the formation of stable Au nanoparticle suspensions with toluene (i.e., Figure 1). However, the surfactant organics are essentially burnt away at higher temperatures (e.g., 200–300 °C), accompanied with fusion of the pristine Au nanoparticles. In accordance with the FTIR results, our CHNS analysis in Table 1 also reveals the same trend of reduction in surface-capping organics. The XPS results of Figure 3b show that the Au 4f_{7/2} and 4f_{5/2} photoelectrons have the binding energies (BEs) of alkanethiol-capped Au⁰ at 83.9 and 87.6 eV,⁹ while the tiny components at 84.8 and 88.3 eV indicate a small degree of charge transfer from the gold to the thiol ends. As expected, the BEs of S 2p_{3/2} and 2p_{1/2} at 162.0 and 163.3 eV are the typical values for the adsorbed thiols on Au,⁹ and sulfate ions (S 2p_{3/2} and 2p_{1/2} at 168.5 and 169.4 eV; Figure 3c) were found on the Au when the alkanethiol was oxidized during the heating in laboratory air.

Figure 4 gives two representative HRTEM images of the self-assembled Au chains. High crystallinity (i.e., clear lattice fringes can be observed, $d_{111} = 0.24 \pm 0.01$ nm) of the Au nanoparticles is generally confirmed, although the decahedral-type structure can also be found. The constant interparticle space is ca. 1.8 nm, indicating an interpenetration of the anchored DT molecules in this line assembly. It seems that all the Au nanoparticles are randomly oriented and there is no strict requirement for crystal orientation in such 1D alignments. Our present approach appears to be able to circumvent a number of technical dilemmas in the template-assisted methods.² For example, controlling interparticle distance is a major drawback in phospholipids, polyelectrolytes, and biomolecule-assisted 1D Au assemblies, while

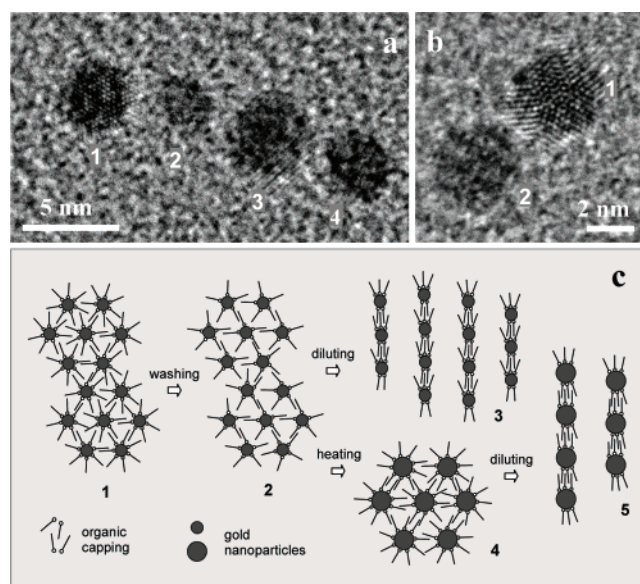


Figure 4. HRTEM images (a,b) of the 150 °C-heated sample: (a-1) a particle viewed along [111] axis, (a-3 and a-4) lattice fringes of d_{111} viewed with a tilted angle, (b-1) a fivefold symmetry seen on a decahedral particle, (a-2,b-2) two randomly oriented particles. The process flowchart (c) of this work: (1) as-prepared nanoparticles, (2) partial removal of surface organics, (3) assemblies of the washed sample, (4) the heat-assisted particle growth, and (5) parallel 1D assembly of larger particles. The organic surfactants refer to DT-molecules, and TOAB is not shown in this illustration.

preparing single-stranded Au nanoparticle chains is extremely difficult using nanotube templates because of their large radial dimensions and nonspecific adsorption sites.² Furthermore, the intricacy among the Au chains resulting from the macromolecular or supramolecular templating techniques can be significantly reduced with our present method.

On the basis of the above results, a process flow chart is summarized in Figure 4c. In general, heat-treated Au nanoparticles can give better 1D assembling results (Figure 1), although short Au strings have also been attained in the washed sample without heat treatment (Supporting Information, SI-3). It should

be mentioned that the molar ratio of TOAB/DT is about 2:1 (deduced from the contents of N and S; Table 1) in the as-prepared sample. However, TOAB has been significantly reduced after ethanol washing, and the resultant surface composition (the molar ratio of TOAB/DT \approx 1:5, deduced from Table 1) does not change essentially even after heat treatment at 150 °C. The better results observed in the heat-treated sample can thus be attributed to a balance between optimal Au particle size and optimal number of surfactant molecules for linear engagement. It is also believed that, in order to maximize van der Waals interaction among their long aliphatic ends, the limited capping surfactants (DT) will accumulate themselves on the two opposite sides of a Au particle (i.e., steps 2 to 3 and steps 4 to 5, Figure 4c), considering also possible synergetic action (such as solvation effect) from the nonpolar solvent molecules to the capping ligands in this relocation process. It is noted that, in order to generate the parallel unidirectional line engagement, there must be repulsive electrostatic forces among the Au strings (existing in less DT-covered portions). Herein, we propose a possible mechanism. While the longer DT molecules are relocating, the positive quaternary amine headgroup and its counterion (Br^-) of the shorter TOAB left behind may become less screened. The resultant charge redistribution along the sideways may thus contribute to the lateral engagement among the neighboring Au strings via Coulomb repulsive interactions. The actual location of the solvated bromide ion, whether in close proximity to the positive headgroup or far from surface of the Au nanoparticle, is clearly a challenging topic in determining the sign of charge repulsion. A more detailed investigation on the actual mechanism will be carried out in our future work.

Conclusions

In summary, for the first time, we have identified key process parameters to generate parallel unidirectional 1D assemblies of gold nanoparticles with the assistance of organic surfactants. By controlling the surfactant population, metal particle size, and amount of solvent for dispersion, the length of nanoparticle chains and their interchain space can be further tailored. In principle, the general findings of this work can also be extended to large-scale 1D organization of other transition/noble metal nanoparticles using simple organic surfactants.

Acknowledgment. The authors gratefully acknowledge the financial support of the Ministry of Education, Singapore.

Supporting Information Available: FESEM, STEM, TEM, and FTIR results. This material is available free of charge via the Internet at <http://pubs.acs.org>.

References and Notes

- (1) (a) Bezryadin, A.; Dekker, C.; Schmid, G. *Appl. Phys. Lett.* **1997**, *71*, 1273–1275. (b) Bezryadin, A.; Westervelt, R. M.; Tinkham, M. *Appl. Phys. Lett.* **1999**, *74*, 2699–2701. (c) Tang, Z. Y.; Kotov, N. A.; Giersig, M. *Science* **2002**, *297*, 237–240. (d) Pacholski, C.; Kornowski, A.; Weller, H. *Angew. Chem., Int. Ed.* **2002**, *41*, 1188–1191. (e) Cho, K.-S.; Talapin, D. V.; Gaschler, W.; Murray, C. B. *J. Am. Chem. Soc.* **2005**, *127*, 7140–7147. (f) Liu, B.; Zeng, H. C. *J. Am. Chem. Soc.* **2005**, *127*, 18262–18268.
- (2) (a) Bae, A.-H.; Numata, M.; Hasegawa, T.; Li, C.; Kaneko, K.; Sakurai, K.; Shinkai, S. *Angew. Chem., Int. Ed.* **2005**, *44*, 2030–2033. (b) Deng, Z. X.; Tian, Y.; Lee, S.-H.; Ribbe, A. E.; Mao, C. D. *Angew. Chem., Int. Ed.* **2005**, *44*, 3582–3585. (c) Minko, S.; Kiriy, A.; Gorodyska, G.; Stamm, M. *J. Am. Chem. Soc.* **2002**, *124*, 10192–10197. (d) Burkett, S. L.; Mann, S. *Chem. Commun.* **1996**, 321–322. (e) Correa-Duarte, M. A.; Liz-Marzán, L. M. *J. Mater. Chem.* **2006**, *16*, 22–25. (f) Gao, X. Y.; Djalali, R.; Haboosheh, A.; Samson, J.; Nuraje, N.; Matsui, H. *Adv. Mater.* **2005**, *17*, 1753–1757. (g) Fresco, Z. M.; Freché, J. M. J. *J. Am. Chem. Soc.* **2005**, *127*, 8302–8303. (h) Huang, J. X.; Tao, A. R.; Connor, S.; He, R. R.; Yang, P. D. *Nano Lett.* **2006**, *6*, 524–529. (i) Guan, Y. F.; Pedraza, A. *J. Nanotechnology* **2005**, *16*, 1612–1618. (j) Yatsui, T.; Nomura, W.; Ohtsu, M. *IEICE Trans. Electron.* **2005**, *E88-C*, 1798–1802.
- (3) (a) Lin, S.; Li, M.; Dujardin, E.; Girard, C.; Mann, S. *Adv. Mater.* **2005**, *17*, 2553–2559 and the references therein. (b) Dirix, Y.; Bastiaansen, C.; Caseri, W.; Smith, P. *Adv. Mater.* **1999**, *11*, 223–227.
- (4) (a) Yin, M.; O'Brien, S. *J. Am. Chem. Soc.* **2003**, *125*, 10180–10181. (b) Zeng, H.; Rice, P. M.; Wang, S. X.; Sun, S. H. *J. Am. Chem. Soc.* **2004**, *126*, 11458–11459.
- (5) (a) Ohara, P. C.; Heath, J. R.; Gelbart, W. M. *Angew. Chem., Int. Ed. Engl.* **1997**, *36*, 1077–1080. (b) Nikoobakht, B.; Wang, Z. L.; El-Sayed, M. A. *J. Phys. Chem. B* **2000**, *104*, 8635–8640. (c) Demers, L. M.; Park, S.-J.; Taton, A.; Li, Z.; Mirkin, C. A. *Angew. Chem., Int. Ed.* **2001**, *40*, 3071–3073. (d) Hassenkam, T.; Nørgaard, K.; Iversen, L.; Kiely, C. J.; Brust, M.; Bjørnholm, T. *Adv. Mater.* **2002**, *14*, 1126–1130. (e) Teranishi, T.; Hasegawa, S.; Shimizu, T.; Miyake, M. *Adv. Mater.* **2001**, *13*, 1699–1701. (f) Shimizu, T.; Teranishi, T.; Hasegawa, S.; Miyake, M. *J. Phys. Chem. B* **2003**, *107*, 2719–2724. (g) Kanehara, M.; Oumi, Y.; Sano, T.; Teranishi, T. *J. Am. Chem. Soc.* **2003**, *125*, 8708–8709. (h) Jin, R. C.; Egusa, S. J.; Scherer, N. F. *J. Am. Chem. Soc.* **2004**, *126*, 9900–9901. (i) Liz-Marzán, L. M.; Mulvaney, P. *J. Phys. Chem. B* **2003**, *107*, 7312–7326.
- (6) Dumestre, F.; Chaudret, B.; Amiens, C.; Renaud, P.; Fejes, P. *Science* **2004**, *303*, 821–823.
- (7) Fan, H. Y.; Leve, E.; Gabaldon, J.; Wright, A.; Haddad, R. E.; Brinker, C. F. *Adv. Mater.* **2005**, *17*, 2587–2590.
- (8) Brust, M.; Walker, M.; Bethell, D.; Schiffrin, D. J.; Whyman, R. *J. Chem. Soc., Chem. Commun.* **1994**, 801–802.
- (9) Li, J.; Zeng, H. C. *Angew. Chem., Int. Ed.* **2005**, *44*, 4342–4345.